JOURNAL OF GEOPHYSICAL RESEARCH, VOL. 108, NO. D15, 8630, doi:10.1029/2002JD002679, 2003

An observational study of drizzle formation in stratocumulus clouds for general circulation model (GCM) parameterizations

Hanna Pawlowska
Institute of Geophysics, Warsaw University, Warsaw, Poland

Jean-Louis Brenguier
Centre National de Recherche Météorologique (CNRM), Météo-France, Groupe d'étude de l'Atmosphère Météorologique (CNRS-GAME), Toulouse, France

Received 20 June 2002; revised 14 September 2002; accepted 29 January 2003; published 7 August 2003.

[1] Climate model parameterization of precipitation formation in boundary layer stratocumulus clouds is a challenge that needs to be carefully addressed for simulations of the aerosol impact on precipitation and on cloud life time and extent, the so-called second indirect effect of aerosol on climate. Existing schemes are generally tuned against global observations of the liquid water path, as very few in situ observations are available for their validation. This issue is addressed here with data collected during the second Aerosol Characterization Experiment. The methodology is different from previous experimental studies in the sense that each case study is first analyzed for retrieving properties that are representative of the observed cloud system as a whole, such as the cloud system geometrical thickness, droplet concentration, precipitation flux, etc. Special attention is given to the characterization of the droplet number concentration by deriving a value that is representative of the aerosol activation process instead of the mean value over the cloud system. The analysis then focuses on the variability of these cloud system values for eight case studies with different aerosol backgrounds. The data set reveals that precipitation forms when the maximum mean volume droplet radius in the cloud layer reaches values >10 μm, the same critical value as previously used in cloud resolving models. This maximum radius can be predicted with an adiabatic diagnostic on the basis of cloud geometrical thickness and droplet number concentration. The measured reduction rate of drizzle water content by precipitation is also compared to predictions of auto-conversion and accretion production rates derived from existing bulk parameterizations initialized with the measured values of cloud droplet and drizzle water content. The good agreement with the parameterizations suggests that the cloud layer reaches a nearly steady state characterized by a balance between the production and reduction rates of cloud and drizzle water content. Finally, it is shown that the cloud system precipitation rate can be expressed as a power law of cloud geometrical thickness and cloud droplet number concentration, hence providing a simple large-scale parameterization of the precipitation process in boundary layer clouds. *INDEX TERMS:* 0320 Atmospheric Composition and Structure: Cloud physics and chemistry; 1610 Global Change: Atmosphere (0315, 0325); 3307 Meteorology and Atmospheric Dynamics: Boundary layer processes; 3354 Meteorology and Atmospheric Dynamics: Precipitation (1854); *KEYWORDS:* aerosol indirect effect, drizzle, stratocumulus, parameterization, general circulation model

Citation: Pawlowska, H., and J.-L. Brenguier, An observational study of drizzle formation in stratocumulus clouds for general circulation model (GCM) parameterizations, *J. Geophys. Res.*, *108*(D15), 8630, doi:10.1029/2002JD002679, 2003.

1. Introduction

[2] The second aerosol indirect effect refers to the possible link between aerosol, more precisely cloud condensation nuclei (CCN), warm cloud precipitation formation, and its impact on cloud lifetime and extent. When added to the natural background aerosol, anthropogenic CCN may cause an increase of the cloud droplet number concentration (CDNC), and, at constant liquid water content (LWC), a decrease of the droplet size. These modifications of cloud microphysical properties promote an increase in cloud albedo [*Twomey*, 1977]. This is generally referred to as the first indirect effect of aerosol on climate. *Albrecht* [1989] pointed out that a decrease of the droplet size is also likely to impact warm cloud precipitation formation. If projected to the global extent of marine stratocumulus cloud systems, this phenomenon, commonly referred to as the

0148-0227/03/2002JD002679$09.00

second indirect effect of aerosol on climate, may substantially alter the water mass budget of stratocumulus, and thus alter their persistence, albedo, and perhaps global climate.

[3] There are however serious obstacles to the parameterization of the stratocumulus precipitation process in climate models. When observed from above, a stratocumulus layer has often the appearance of a homogeneous system, but remote sensing of its internal structure with a radar [*Vali et al.*, 1998] reveals in fact a very heterogeneous organisation of the precipitation. Cloud resolving models (CRM), with a spatial resolution of a few tens of meters and explicit microphysical schemes [*Feingold et al.*, 1994; *Kogan et al.*, 1995], are able to simulate the internal dynamical structure of a stratocumulus and the resulting microphysical structure. Simpler "bulk" parameterizations have been derived from explicit microphysical schemes [*Tripoli and Cotton*, 1980; *Beheng*, 1994; *Khairoutdinov and Kogan*, 2000] (hereinafter referred to as *TC80*, *B94*, and *KK00*, respectively), in which the complexity of the hydrometeor distribution is reduced to a set of two or three parameters. *KK00* mentioned in particular that "their scheme cannot be simply extrapolated for use in larger-scale models since the derived water conversion rates depend nonlinearly on local (eddy scale) cloud variables." Nevertheless the parameterization schemes of precipitation formation that are presently used in general circulation models (GCM) are directly transposed from such CRM bulk parameterizations [*Tiedtke*, 1993; *Lohmann and Roeckner*, 1996; *Fowler et al.*, 1996; *Ghan et al.*, 1997; *Rotstayn*, 1997; *Wilson and Ballard*, 1999], although a GCM is limited to a horizontal resolution of 50 to 200 km and a vertical resolution of typically 100 m.

[4] The GCM schemes are generally tuned against global monitoring of clouds and precipitations [*Rotstayn*, 2000]. A different and complementary approach is to test the parameterizations against data collected in the field. In contrast to global monitoring a field experiment reflects a limited subset of the global climate, but it provides information upon the values of the input and output parameters of the numerical schemes, hence allowing separate examination of the various pieces that are assembled in a GCM parameterization. Such data sets however are scarce when focusing on boundary layer precipitation at the mesoscale. CLOUDYCOLUMN, one of the five projects in the Second Aerosol Characterization Experiment (ACE-2), is particularly suited because it comprises eight case studies that have been sampled over an area of about 60 × 60 km, and thus allows the characterization of physical parameters that are representative of the GCM spatial resolution. Particular attention is given in the data analysis to the resolution scale issue with regard to the nonlinearity of the physical processes involved in the formation of precipitation. Another interesting feature of this campaign is the variety of the observed aerosol backgrounds, hence of the CDNC values, with very different resulting precipitation rates. This campaign is therefore unique for the examination of the impact of the aerosol on precipitation formation.

2. Theoretical Background and Methodology

[5] Precipitation in warm convective clouds proceeds in three stages. First, cloud condensation nuclei are activated in response to supersaturation produced in an updraft, mainly at cloud base. The so-called activation process that determines the initial CDNC value in a convective cell is discussed by *Guibert et al.* [2003] and *Snider et al.* [2003], in this special section. Second, droplets formed on activated nuclei, with a size of about 1 μm, grow by vapor diffusion in the convective cell. The droplet growth rate being inversely proportional to the droplet size, small droplets are growing faster than the big ones and the droplet spectrum becomes narrower with altitude [*Brenguier and Chaumat*, 2000]. The third and last stage involves collision between cloud particles and their coagulation, also referred to as collection [*Berry*, 1967; *Bartlett*, 1970]. Droplets with a radius smaller than 6 μm have a negligible probability of coagulation. Above that size, the probability increases sharply with the droplet radius (the collection kernel varies approximately as r^6, in the droplet radius range r between 10 and 50 μm [*Pruppacher and Klett*, 1997]). The transition from condensation to collection growth therefore requires the presence of a few big droplets, also called precipitation embryos. Their origin is still a controversial issue possibly involving, in addition to the current theory of condensational growth, the influence of giant CCN [*Feingold et al.*, 1999a], in-cloud turbulence [*Feingold et al.*, 1999b], and the radiative impacts on droplet growth by vapor diffusion [*Harrington et al.*, 2000].

[6] The combination of the three stages mentioned above generally results on the following scenario for the particle spectrum. On a radius scale, the particle growth rate starts with a maximum during activation and decreases with increasing radius (condensation process). A minimum is reached at about 20 μm that corresponds to the transition between the condensation and the collection processes. At larger radius values the growth rate by collection increases and the droplet sizes are only limited by drop internal instability leading to their breakup. Particle breakup is not discussed here as it does not play a significant role in stratocumulus clouds. It follows that most of the observed hydrometeor spectra show very few particles at radius values around 20 μm. It is thus common to designate particles smaller than 20 μm as droplets, while the bigger ones are referred to as drops.

[7] Because the explicit representation of the whole particle spectrum in multidimensional numerical models is expensive (25 size classes as given by *Feingold et al.* [1994]; 44 size classes as given by *Kogan et al.* [1995]), "bulk" parameterizations have been developed. Following *Kessler* [1969], the spectrum may be divided in two categories: cloud droplets, having negligible terminal velocities, and cloud drops with significant terminal velocities. The collection process can then be parameterized with two simpler processes: the self collection of cloud droplets (auto-conversion), and the collection of small droplets by large drops (accretion). Note nevertheless that auto-conversion is an artifact of the droplet spectrum separation in two categories. At the initial stage, all the particles produced by CCN activation and condensational growth are smaller than 20 μm and as such belong to the droplet category. The initial drop concentration is null, so that accretion cannot be initiated. Auto-conversion generates the initial drop water content that can then activate the accretion process. A second artifact of the bulk parameter-

ization is the formulation of a threshold for auto-conversion, expressed either in term of droplet critical water content [*Kessler*, 1969] or droplet critical radius [*TC80*], which accounts for the nonlinearity of the collection process mentioned above, at the transition between droplets and drops.

[8] The use of a bulk parameterization allows the number of microphysical variables to be reduced to two, the droplet water content, q_c, and the drop water content q_r. CDNC is an optional third variable to account for the impact of aerosol on cloud microphysics. Power law relationships have been established for the water content conversion rates between droplets and drops, which were tuned against explicit simulations of the collection process [*TC80*; *B94*; *KK00*].

[9] The bulk parameterization concept has been extended to the large scale, with q_c as a prognostic variable, while q_r is generally diagnosed as done by *Tiedtke* [1993], *Lohmann and Roeckner* [1996], *Ghan et al.* [1997], *Rotstayn* [1997], or *Wilson and Ballard* [1999], for using a longer time step than a prognostic treatment of precipitation [*Fowler et al.*, 1996] would allow. The auto-conversion schemes are taken from *Sundqvist* [1978] (with a critical water content) or from *TC80* or *B94* (with a critical droplet radius). When q_r is diagnosed, accretion is accounted for by either correcting the auto-conversion scheme as in *Tiedtke* [1993] and *Rotstayn* [1997], or calculated according to *B94* with the diagnosed rainwater content.

[10] The auto-conversion critical radius, r_0, used in a GCM is a very uncertain parameter [*Rotstayn*, 1999], which can be tuned by comparing the simulations with satellite monitoring of the liquid water path (LWP) [*Rotstayn*, 2000], while in CRM its value is derived from comparison with explicit microphysics calculations [*TC80*]. It is thus common to use smaller r_0 values in GCM, from 4.5 to 7.5 μm [*Boucher and Lohmann*, 1995; *Rasch and Kristjansson*, 1998; *Rotstayn*, 1999], than in CRM, where typically 10 μm is the accepted threshold [*TC80*]. This difference accounts for the coarse spatial resolution of the GCM as compared to the CRM. The onset of precipitation is in fact particularly sensitive to the subgrid GCM cloud scheme, which can generate very different LWC peak values from the same grid mean LWC. The resulting variability of the predicted second aerosol indirect effect is dramatic [*Rotstayn*, 2000; *Menon et al.*, 2002].

[11] Two issues are crucial in our experimental approach: the resolution scale and the predictability of the parameters selected for parameterizing the precipitation process. *Pawlowska and Brenguier* [2000] described rigorous statistical procedures for characterizing each ACE-2 case study with values of geometrical thickness H and droplet concentration N_{act}, that are representative of the cloud system at the 60 km scale. We further consider that this scale represents a GCM grid. *Brenguier et al.* [2000a] and *Schüller et al.* [2003] demonstrate that cloud radiative properties at the cloud-system scale are determined by these two parameters. *Snider and Brenguier* [2000], and *Guibert et al.* [2003] and *Snider et al.* [2003] in this special section, reveal that the CDNC value predicted with a detailed CCN activation model, initialized with the aerosol physicochemical properties that were measured at the ACE-2 surface site, overestimates N_{act} by a factor that varies between 30 and 90%. We nevertheless assume that parameterizations, such as the one described by *Zhang et al.* [2002] if initialized with aerosol physicochemical properties predicted by an aerosol transport model, shall be able to correctly diagnose N_{act} in each GCM grid. As for the other processes involved in the aerosol indirect effect, that are discussed in this special section, our methodology is thus based on the assumption that H and N_{act} can be predicted (either diagnostic or prognostic) in the cloudy fraction of each GCM grid, and that other microphysical processes can be parameterized at the GCM grid scale using these two parameters only. An alternative for characterizing the observed CDNC could be to derive its mean value from the whole data set. Such a mean value is lower than N_{act} because of dilution by mixing and drizzle scavenging. CRM simulations however show that precipitation starts in the core of the convective cells, where CDNC is closer to N_{act} rather than to the mean CDNC value, that also accounts for the diluted cloud regions. In addition, there is presently no scheme for diagnostic of the mean CDNC, which would require a better understanding of the mixing and drizzle scavenging processes.

[12] The eight ACE-2 case studies are first examined at the small scale (~100 m) in order to characterize the spatial heterogeneity of the precipitation fields and the impact of drizzle on droplet size and concentration. Three features of the precipitation process and of its parameterization are then addressed with the ACE-2 data set.

[13] 1. Auto-conversion threshold (section 5.1): Does the ACE-2 data set show a relationship between N_{act} and the formation of precipitation? Does this relationship exhibit a threshold? Can this threshold be expressed in term of the two cloud-system scale parameters H and N_{act}? Can we evaluate with the data set a good approximation of the critical threshold value?

[14] 2. Existing parameterization schemes (section 5.2): Are the auto-conversion and accretion schemes still valid when used with grid scale averaged values of the droplet and drop water contents, despite their inherent nonlinearity?

[15] 3. Grid scale diagnostic of the precipitation rate (section 5.3): Does the data show a power law relationship between (H, N_{act}) and the grid scale averaged precipitation rate?

3. Parameterization of Cloud Microphysics

[16] Parameterizations of the condensation and collection processes are briefly summarized in the next two subsections. The equations are in SI units (unless stated differently), although values of the microphysical variables discussed in the text are (conversion factor to SI in parenthesis) in μm (10^{-6}) for droplet radius, cm^{-3} (10^{6}) for CDNC, $g\ m^{-3}$ (10^{-3}) for LWC, $g\ m^{-2}$ (10^{-3}) for LWP and $g\ m^{-2}\ s^{-1}$ (10^{-3}) for the precipitation flux.

[17] Note that cloud and drizzle observed values are expressed in this paper in term of water content ($g\ m^{-3}$), while parameterizations discussed hereinafter rather use mixing ratio (g/kg). For the eight cloud systems documented in the paper, the air density was in fact slightly greater than unity, by about 3% in average and 7% at the maximum. This conversion factor has been neglected with

regard to the uncertainty in water content measurements, of 30% for cloud water and 40% for drizzle water.

3.1. Condensation Process

[18] *Pawlowska and Brenguier* [2000] and *Brenguier et al.* [2000a] have shown that the cloud microphysical properties of the stratocumulus clouds observed during ACE-2 were realistically simulated with the adiabatic cloud model, that relates droplet size to CDNC and height above cloud base h.

[19] In an adiabatic parcel the cloud droplet number concentration N is constant and LWC increases linearly with altitude above cloud base h. The adiabatic mean volume radius r_{vad} of the droplet size distribution can thus be derived from

$$\frac{4\pi}{3}\rho_w N r_{vad}^3 = q_{ad}(h) = C_w h, \tag{1}$$

where C_w, also referred to as the condensation coefficient, depends on the temperature and pressure at cloud base [*Brenguier*, 1991]. The maximum r_{vad} value

$$r_{vad}(H) = \left(C_w H \Big/ \frac{4\pi}{3}\rho_w N \right)^{1/3} \tag{2}$$

is reached at cloud top, where H is the cloud geometrical thickness. This maximum adiabatic size will further be used as a reference to compare with the mean volume droplet radius (MVDR) values derived from the measured droplet size distributions. The following formulae result for the cloud layer vertically averaged adiabatic LWC, $\overline{q_{ad}}$:

$$\overline{q_{ad}} = \frac{1}{2} C_w H, \tag{3}$$

and the liquid water path W_{ad}:

$$W_{ad} = \frac{1}{2} C_w H^2. \tag{4}$$

Since the temperature and pressure at cloud base did not vary significantly during ACE-2, C_w is hereinafter assumed constant (2×10^{-6} kg m^{-4}).

3.2. Bulk Parameterization of Collection

[20] Bulk parameterizations of the collection process are based on the above mentioned separation between droplets and drops, represented by their respective water contents, q_c (for cloud water) and q_r (for rainwater). The parameterizations are expressed as power laws of these bulk variables after tuning against results of explicit microphysical models applied over a large range of conditions typical of convective clouds [*TC80*; *B94*]. The rate of droplet collection by raindrops, also referred to as the accretion rate, was formulated as

$$(dq_r/dt)_{acc} = C_{acc} q_c q_r \quad \text{with } C_{acc} \approx 6. \tag{5}$$

The same exercise, but more specifically focused on stratocumulus [*KK00*] led to slightly different values of the accretion coefficient, $C_{acc} \approx 3.7$, or even a different power law (hereafter referred to as their "best fit"), namely,

$$(dq_r/dt)_{acc} = 67(q_c q_r)^{1.15}. \tag{6}$$

The onset of precipitation is accounted for by an additional process that describes the self-collection of droplets, also referred to as the auto-conversion process. Formulation by *TC80* was as follows:

$$(dq_r/dt)_{aut} = C_{aut} N^{-1/3} q_c^{7/3} H(r_{vc} - r_0) \quad \text{with } C_{aut} \approx 3 \times 10^3, \tag{7}$$

while *B94* proposed a different power law ($N^{-3.3} q_c{}^{4.7}$). *KK00*, for the stratocumulus case, found a smaller value of the auto-conversion coefficient, C_{aut} = 220, though the "best fit" was obtained with a different power law:

$$(dq_r/dt)_{aut} = C_{aut} N^{-1.79} q_c^{2.47} \mathcal{H}(r_{vc} - r_0) \quad \text{with } C_{aut} \approx 7.4 \times 10^{13}. \tag{8}$$

In these formulae, $\mathcal{H}$ is the Heaviside step-function and r_0 is the auto-conversion critical radius, whose value is generally set to 10 μm in CRM bulk parameterizations.

[21] Part of the difference between the results of *TC80* and *B94*, on the one hand, and those of *KK00*, on the other hand, is attributable to the range of variations of the parameters selected for the characterization of the cumulus case, for the first two references, against the stratocumulus case, for the third one. However, differences in the parameterization of the auto-conversion process, that are larger than for the accretion process, also arise from the fact that auto-conversion is an artifact of the bulk parameterization concept, and that its contribution is only significant at the early stage of precipitation formation. After drop water content has been produced by auto-conversion, the accretion process contributes more efficiently to the transfer of cloud water into rainwater. This feature of the bulk parameterization reflects the fact that the collection of droplets by drops is more efficient at depleting cloud water content than the droplet self-collection. *Beheng*'s [1994] calculations with an initial cloud water content of 1 g m^{-3} reveal that the accretion rate becomes larger than the auto-conversion rate (at a value of $\sim 10^{-4}$ g m^{-3} s^{-1}) within 100 to 500 s of simulation, depending on the width of the initial droplet spectrum.

[22] Such bulk parameterizations are suited for CRM because they allow detailed description of the various stages of precipitation formation, namely the formation of precipitation embryos at the level where the auto-conversion threshold value of the droplet radius is reached, and the progressive conversion of cloud water into rainwater by collection. These parameterizations utilize a time step of a few seconds that is consistent with the spatial resolution of the models and the characteristic time of the processes. Because auto-conversion and accretion formulations are nonlinear, it is important to restrict their application to simulations where local values of the liquid water content are explicitly predicted [*K00*].

[23] The transposition of such parameterizations to GCM, with a coarse spatial resolution, is therefore questionable. In

particular, constants such as the auto-conversion critical radius and the auto-conversion and accretion coefficients are often adjusted to account for the smoothing effect of the GCM spatial resolution on local peak values of the microphysical parameters [*Fowler et al.*, 1996; *Rotstayn*, 1997, 2000]. It is not evident either that they are appropriate in term of efficiency. In fact, the simulations mentioned above indicate that the transition from auto-conversion to accretion is achieved within 500 s, a period of time shorter than a typical GCM time step. This suggests that quasi-steady solutions of the whole process could be more relevant for GCM parameterizations.

4. Data Processing

[24] In the ACE-2 data set, cloud microphysical properties were derived from measurements made on board the Meteo-France Merlin-IV [*Brenguier et al.*, 2000b], with the Fast-FSSP [*Brenguier et al.*, 1998], for the droplet size distribution in the radius range 1.3–18 μm, and the OAP-200X, for the drizzle size distribution in the radius range 10–160 μm. To avoid size range overlap between the Fast-FSSP and the OAP, the first OAP class has not been accounted for, so that the effective OAP range is 20–160 μm. Accurate and robust statistics of the cloud layer properties were derived from the series of ascents and descents that were flown on each mission, from at least 15 profiles on 8 and 17 July, up to 35 profiles on 26 June [*Pawlowska and Brenguier*, 2000]. The data were collected along a 60 km square flight track [*Guibert et al.*, 2003].

[25] Data processing aims at reducing the spatial variability of the measured parameters for the retrieval of values representative of the cloud system as a whole. It is also implicitly assumed that the cloud system properties are stationary along the duration of the mission (typically longer than 3 hours, and centered on local noon time). In the following subsections, special attention is thus given to samples selection and the definition of the so-called cloud-system, or grid scale, representative parameters. The two key parameters are the cloud layer geometrical thickness H and the CDNC representative value N_{act}. H aims at characterizing the thickness of an ideal plane-parallel cloud layer that would exhibit the same mean microphysical and radiative properties as the actual heterogeneous cloud layer. It is assumed that such a parameter can be diagnosed from subgrid parameterizations of the temperature and water vapor spatial distributions [*Lock et al.*, 2000]. N_{act} aims at reflecting the impact of aerosol on cloud microphysics and it is assumed that such a parameter can be predicted using parameterizations of the aerosol activation process, such as described in *Zhang et al.* [2002]. Note that N_{act} cannot be derived by averaging the measured CDNC over the whole sampled cloud system, because the signature of the aerosol activation process is mainly detectable in unmixed convective cells. Additional processes, such as mixing with the overlying dry air and the droplet collection by drizzle, also referred to as drizzle scavenging, further affect the CDNC values, hence shadowing the impact of aerosol on cloud microphysics. The ultimate objective is to diagnose the radiative properties (first indirect effect) and precipitation rate (second indirect effect) from these two parameters only, without any detailed representation of the microphysics. For the analysis of precipitation formation, that is addressed in this paper, two sets of microphysical parameters are considered: (1) cloud droplet liquid water content and droplet sizes and (2) drizzle water content, drizzle drop sizes and precipitation flux.

4.1. Estimation of *H*

[26] Cloud geometrical thickness values were derived for each flight according to the following procedure. The analysis is based on 10 Hz (9 m resolution along the aircraft track) samples of CDNC collected with the Fast-FSSP along ascending and descending profiles through the cloud layer. First, the N cumulative frequency distribution is calculated for each profile separately and the value at 99% probability is referred to as $N_{p\text{-}max}$. Second, the altitude cumulative frequency distribution of the samples, with $N > 0.2\ N_{p\text{-}max}$, is used to define the cloud base altitude, as the altitude value at 1% probability of the distribution. In *Pawlowska and Brenguier* [2000] the cloud base altitude was estimated by fitting the vertical profile of the LWC peak values to the adiabatic prediction. The present procedure produces cloud base altitude estimates slightly higher than the previous one, but by <25 m for each ACE-2 case study. Third, for each separate profile the cloud base altitude is subtracted from the sample altitude to derive the height above cloud base h. Fourth the h cumulative frequency distribution is generated from the complete series of ascents and descents, with samples such that $N > 0.2\ N_{max}$, where N_{max} is the 99th percentile of the CDNC cumulative distribution for the complete series. Finally, the cloud geometrical thickness H is defined as the 98th percentile of the h cumulative distribution.

4.2. Estimation of N_{act}

[27] The definition of the characteristic CDNC value also requires a rigorous approach:

[28] 1. Maximum CDNC values are measured in convective updraft, where they depend upon the CCN properties and the updraft speed at cloud base [*Snider and Brenguier*, 2000; *Snider et al.*, 2003]. Close to cloud top CDNC is often affected by mixing with the overlying dry air. The estimation of CDNC is thus restricted to unmixed (quasi-adiabatic) samples collected at an altitude lower than $0.6\ H$.

[29] 2. When drizzle drops are present, the observed droplet spectrum is generally broad and extends over both the Fast-FSSP and the OAP-200-X size ranges. The MVDR value is larger than in samples void of drizzle [*Gerber*, 1996] and CDNC is reduced because of droplet scavenging by drizzle drops. Including drizzle samples in the CDNC statistics would result in a significant bias toward lower CDNC and larger MVDR values in cloud systems that are efficiently precipitating, and it would strongly amplify the expected negative correlation between CDNC and precipitation rate. The objective here being to characterize the droplet spectrum just before the onset of precipitation, samples with a detectable drizzle concentration are rejected from the statistics.

[30] 3. Regions close to the cloud base are characterized by small droplets, some of them being smaller than the Fast-FSSP detection threshold (1.3 μm in radius). Therefore samples close to the cloud base $h < 0.4\ H$ are rejected.

[31] In summary, the N frequency distribution is generated with samples such that

$$\text{(i)} q_c(h) > 0.9\, q_{ad}(h) \quad \text{(ii)}\ N_{OAP} < 2\,\text{cm}^{-3} \quad \text{(iii)}\ 0.4\,H < h < 0.6\,H, \tag{9}$$

where N_{OAP} is the drizzle concentration measured using the OAP-200X. The mean value of the N frequency distribution is referred to as N_{act}. Note that in *Pawlowska and Brenguier* [2000], this value was referred to as N_{mean}, but this notation was further considered as ambiguous with regard to the whole area mean CDNC value. The cumulated length of samples collected during ascent or descent, with $0.4\,H < h < 0.6\,H$, is referred to as L_N. The fraction of those samples where criteria (i) and (ii) are verified is designated by F_N.

4.3. Estimation of LWC and the Droplet Sizes

[32] The complete series of ascents and descents flown by the Merlin-IV are used to calculate the mean LWC over the cloudy fraction of the sampled layer (vertically and horizontally averaged) that is designated by q_c. Horizontal legs are not taken into account because the droplet properties are strongly stratified in the vertical. Horizontal legs would thus introduce a bias in the statistics toward values specific of the altitude level of the leg. Two size parameters are then derived from the measured size distributions: the mean volume radius r_v, that can be compared to the adiabatic prediction, and the value at the 95th percentile of the cumulative size distribution, r_{95}, that characterizes the size of the biggest droplets in a spectrum. The cumulative frequency distributions of r_v and r_{95} are generated from the complete series of ascents and descents for each mission ($0 < h < H$). Samples with $q_c(h) < 0.9\, q_{cad}(h)$ are rejected to avoid underestimation due to mixing and droplet evaporation, and samples with $N_{OAP} > 2\ \text{cm}^{-3}$ are rejected to avoid overestimation due to the counting of drizzle drops in the Fast-FSSP range. In contrast to the CDNC statistics, samples collected at cloud top are not rejected in order to capture the biggest droplets that formed near cloud top. The cumulated length of samples collected during ascent or descent, with $0 < h < H$, is referred to as L_c. The values at 98% probability of the r_v and r_{95} cumulative frequency distributions are defined as the maximum MVDR value, r_{vmax}, and the maximum 95th percentile, r_{95max}, respectively. Finally the cloud fraction F_c is defined as the percentage of samples collected along L_c, with $N > 5\ \text{cm}^{-3}$.

4.4. Estimation of Drizzle Properties

[33] Because of the small sample volume of the OAP-200X with regard to the drizzle concentration, drizzle measurements are based on 1 Hz samples, instead of the 10 Hz sampling used for droplet measurements. Drizzle properties are derived from all the cloud samples, including horizontal legs. The rationale for using horizontal leg measurements is twofold. First, drizzle particles are not numerous and the statistical significance of their measurements is low compared to droplet measurements. Horizontal legs provide additional data, hence better statistics. Second, oversampling of a specific level is less a concern for drizzle particles because their properties are less stratified in the vertical than droplet properties are, as shown by the vertically stratified statistics in *Brenguier et al.* [2003]. The cumulated length of samples collected during ascents, descents and horizontal legs, with $0 < h < H$, is referred to as L_r, and the drizzle fraction F_r is defined as the percentage of samples collected along L_r, with $N_{OAP} > 2\ \text{cm}^{-3}$.

[34] The maximum drizzle concentration in the cloud layer, N_{OAPmax}, is defined as the 90th percentile of the measured N_{OAP} cumulative frequency distribution. The mean cloud system drizzle water content (g m^{-3}), designated by q_r, and mean drizzle flux (g m^{-3} s^{-1}), designated by R, are derived from the 1 Hz measured OAP size distribution, and then averaged over the cloudy fraction of the sampled area:

$$q_r = \left\langle \frac{4}{3}\pi\rho_w 10^{-9} \sum n_i r_i^3 \right\rangle \tag{10a}$$

and

$$R = \left\langle \frac{4}{3}\pi\rho_w 10^{-9} \sum n_i r_i^3 v_i \right\rangle, \tag{10b}$$

where the symbol $\langle\ \rangle$ designates the mean value over L_r, and n_i (cm^{-3}) is the 1 Hz measured OAP drop concentration in the size class i, which is characterized by a drop radius r_i (μm) and a drop terminal velocity v_i (m s^{-1}) [*Pruppacher and Klett*, 1997]:

$$v_i = \eta_a \text{Re} \Big/ 2\rho_a r, \tag{11}$$

where η_a is the dynamic viscosity of air, Re is the Reynolds number, and ρ_a is the air density. This formula holds for drizzle drops with a radius between 10 and 500 μm. In the range from 10 to 30 μm the terminal velocity varies in proportion to r^2, while it increases almost linearly with r at larger values. R represents a flux of precipitating water content through the cloud layer; hence it does not strictly reflect the precipitation rate at the surface. The vertical resolution of a GCM is too coarse for simulating the vertical advection of precipitation in a boundary layer cloud that generally occupies one or two model layers. For calculation of the water budget over the whole cloud layer, the vertical flux is therefore transformed into a drizzle water content reduction rate by precipitation (g m^{-3} s^{-1}) by assuming R is uniform over the cloud layer thickness: $(dq_r/dt)_{prec} = R/H$.

4.5. Data Summary

[35] The results of the data processing are reported in Table 1. The four first rows are relevant to H and N_{act}. These are used for predicting adiabatic LWC, LWP and MVDR at cloud top, with the corresponding sample length L_N and fraction F_N corresponding to quasi-adiabatic, non precipitating samples. The eight ACE-2 cases are sorted according to N_{act}. Following the classification discussed in *Guibert et al.* [2003], based on the aerosol physicochemical properties measured at the surface site and boundary layer air mass origin derived from backward trajectories, the two first cases are referred to as pristine, the next three cases as intermediate, and the three last cases as polluted. The following 6 rows correspond to the droplet properties with the derived parameters r_{vmax}, r_{95max}, q_c, L_c, and F_c, and the adiabatic prediction of MVDR at cloud top $r_{vad}(H)$. The next set of 6

Table 1. Characterization of the Eight ACE-2 Cases[a]

Variable	Units	26 June	25 June	17 July	19 July	16 July	18 July	8 July	9 July
H	m	202	262	272	272	222	192	182	167
N_{act}	m^{-3} ($\times 10^{-6}$)	51	75	114	134	134	178	208	256
L_N	km	14.4	19.8	9.6	14.5	8.7	8.8	8.9	14.1
F_N		0.31	0.22	0.46	0.54	0.52	0.33	0.35	0.29
r_{vmax}	m ($\times 10^6$)	12.6	11.4	10.5	10.5	10.3	8.0	7.5	6.7
r_{95max}	m ($\times 10^6$)	15.9	15.7	14.4	14.3	15.3	11.9	9.7	9.3
$r_{vad}(H)$	m ($\times 10^6$)	12.4	11.9	10.4	9.9	9.2	8.0	7.5	6.8
q_c	kg m^{-3} ($\times 10^6$)	125	137	205	200	162	116	128	110
L_c	km	59.2	84.3	40.6	56.2	37.0	36.5	37.3	50.7
F_c		0.87	0.80	0.88	0.87	0.83	0.75	0.86	0.50
N_{OAPmax}	m^{-3} ($\times 10^{-6}$)	10.5	21.2	5.7	4.3	4.0	0.8	1.6	2.0
q_r	kg m^{-3} ($\times 10^6$)	232	417	189	114	36	0	6	16
R	kg m^{-2} s^{-1} ($\times 10^6$)	25.5	63.3	37.2	25.1	12.0	0	0.75	2.22
$(dq_r/dt)_{prec}$	kg m^{-3} s^{-1} ($\times 10^9$)	127	241	137	92	53	0	4	13
L_r	km	444	377	253	344	362	251	323	435
F_r		0.24	0.22	0.41	0.25	0.06	0	0.03	0.05
$(dq_r/dt)_{aut}TC$	kg m^{-3} s^{-1} ($\times 10^9$)	6.32	6.88	15.33	13.71	8.39	3.50	4.18	2.74
$(dq_r/dt)_{aut}KK1$	kg m^{-3} s^{-1} ($\times 10^9$)	0.46	0.50	1.12	1.01	0.62	0.26	0.31	0.20
$(dq_r/dt)_{aut}KK2$	kg m^{-3} s^{-1} ($\times 10^9$)	0.27	0.17	0.22	0.15	0.09	0.02	0.02	0.02
$(dq_r/dt)_{acc}TC$	kg m^{-3} s^{-1} ($\times 10^9$)	174	343	233	137	35	0	4	11
$(dq_r/dt)_{acc}KK1$	kg m^{-3} s^{-1} ($\times 10^9$)	107	211	143	84	22	0	3	7
$(dq_r/dt)_{acc}KK2$	kg m^{-3} s^{-1} ($\times 10^9$)	144	314	201	109	22	0	2	6

[a]Parameters as defined in section 4 for the first 16 rows and section 5.2 for the last six rows.

rows is relevant to drizzle properties, with the derived parameters N_{OAPmax}, q_r, R, $(dq_r/dt)_{prec}$, L_r, and F_r. The last rows of the table are further discussed in section 5.2.

[36] Note that the characteristic CDNC value (section 4.2), cloud droplet properties (section 4.3), and drizzle properties (section 4.4) are based on different sample lengths, represented by $F_N \times L_N$, L_c, and L_r, respectively. They correspond to different subsamples of the total horizontal distance flown in cloud along the 60 km square pattern. F_c is representative of the cloud fraction over the sampled area.

[37] Note also that the parameters in Table 1 belong to two categories. q_c, q_r, R, and $(dq_r/dt)_{prec}$ are extensive parameters, that are averaged over the entire cloud volume, in order to be comparable to extensive GCM variables used in the water budget. H, N_{act}, r_{vmax}, r_{95max}, and N_{OAPmax} are intensive parameters. N_{act} symbolizes the typical CDNC value resulting from CCN activation, and it is larger than the cloud volume averaged CDNC, that also includes samples affected by mixing or drizzle scavenging. r_{vmax} and r_{95max} represent the maximum radius droplets can reach in a cloud layer of thickness H, and it can be compared to the adiabatic prediction $r_{vad}(H)$. The rationale for using such peak values instead of the cloud volume mean values for comparison with GCM parameterizations arises from the nonlinearity of the droplet collection process. In fact only a few precipitation embryos, over limited cloud areas and time durations, are sufficient for the onset of precipitation that further propagates via insemination of larger cloud volumes by the resulting precipitating drops. For an experimental estimation of the auto-conversion critical radius, the maximum MVDR value that is produced by convective ascent at the top of the layer is therefore more appropriate than the MVDR value averaged over the entire cloud volume.

5. Analysis

5.1. Onset of Precipitation

[38] Figures 1a and 1b illustrate the spatial variability of drizzle in boundary layer clouds, for a pristine (26 June) and a polluted (9 July) case. Each point corresponds to a 1-Hz sample, about 90 m spatial resolution, and it is represented by MVDR and CDNC. The color scale indicates the corresponding number concentration of drizzle particles measured with the OAP. LWC isolines are also reported, with labels corresponding to height above cloud base h, such that $q_c = q_{ad}(h)$. For the 26 June and the 9 July cases the values of cloud geometrical thickness H, are 202 and 167 m, respectively. A few samples show LWC values corresponding to deeper cells. This can be attributed to either measurements performed in the few cells that are deeper than H (2% of the h cumulative distribution), or to drizzle drops that are counted in the FSSP size range.

[39] The two cases exhibit noticeable differences. On 26 June, CDNC values are lower than 100 cm^{-3}, while values up to 300 cm^{-3} are observed on 9 July. MVDR values are smaller than 8 μm in the polluted case, while they reach values larger than 14 μm in the pristine case. As a result, the drizzle concentration stays below 2 cm^{-3} in the polluted case, but it increases to 6 cm^{-3} in the pristine case. The most interesting feature though is the location of the peak values of drizzle concentration. In the polluted case they are associated with large CDNC values, between 200 and 300 cm^{-3}. This suggests that a few large droplets are growing in undiluted cloud cores up to a size measurable with the OAP (20 μm in radius), but that they are inefficient at collecting droplets. In the pristine case they are rather concentrated at CDNC values of the order of half the peak value, around 20 to 50 cm^{-3}. This feature suggests that drizzle particles are efficient at depleting CDNC and transferring cloud to rainwater. This point will be further illustrated with the complete data set.

[40] Figure 2 shows the droplet maximum sizes versus maximum drizzle concentration, N_{OAPmax} for the eight cases. Each case is represented by a symbol and a vertical bar extending from r_{vmax} to r_{95max}. The adiabatic prediction is superimposed. The three most polluted cases (18, 8, and 9 July), with CDNC mean values from 178 to 256 cm^{-3}, are not efficient at producing precipitation (peak drizzle con-

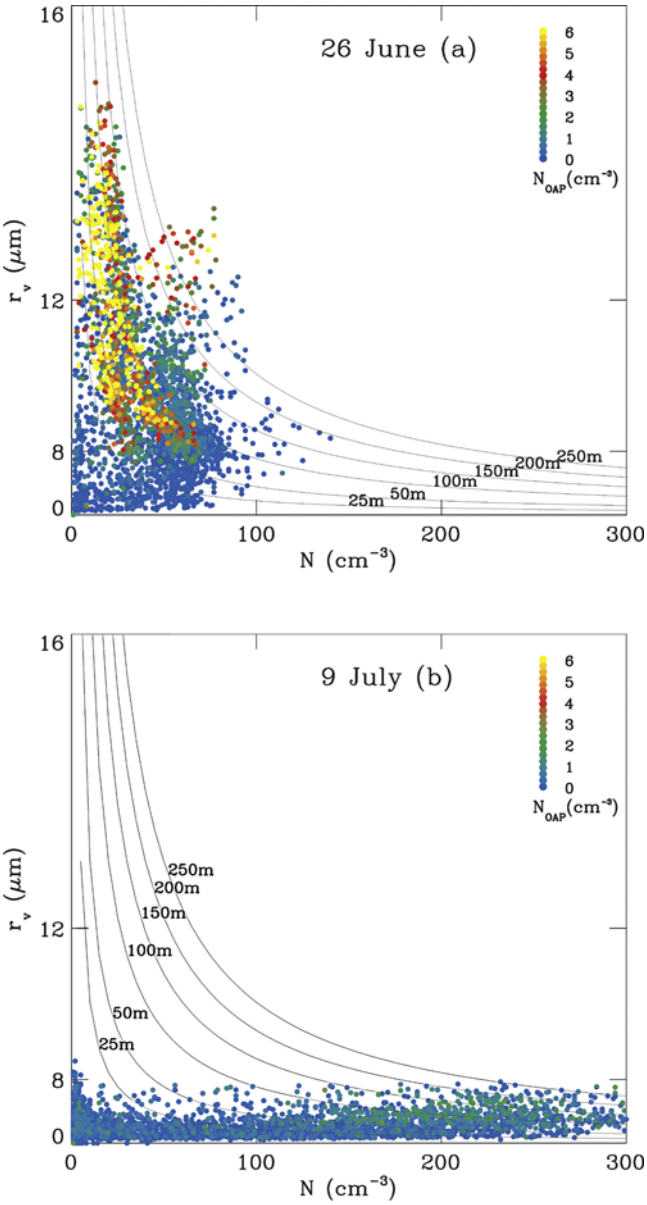

Figure 1. Scatterplot of 1 Hz samples MVDR versus CDNC. The color scale is relative to N_{OAP}, as indicated in the legend. (a) Clean and (b) polluted ACE-2 cases. The isolines represent constant q_c values labeled with h values such that $q_c = q_{ad}(h)$.

centrations smaller than 2 cm^{-3}). In contrast, the two most pristine cases (25 and 26 June), with N_{act} values of 75 and 51 cm^{-3}, respectively, exhibit much larger peak values of drizzle concentration, 21.2 and 10.5 cm^{-3}, respectively. The three intermediate cases (17, 19, and 16 July), with N_{act} values from 114 to 134 cm^{-3}, show also intermediate values of peak drizzle concentration, from 5.7 down to 4 cm^{-3}. The good agreement between the observed and predicted maximum MVDR values demonstrates that both N_{act} and H contribute to the determination of the maximum droplet size, that clearly impacts on the precipitation process. This result in itself constitutes a robust experimental evidence of the second aerosol indirect effect. In particular, it must be noted that an observed negative correlation between N_{act} and N_{OAPmax} only, without any information about H, would not constitute a demonstration, because of the N_{OAPmax} dependence on H. This result also provides an empirical estimation of the auto-conversion critical radius for the onset of precipitation in stratocumulus clouds. The eight analyzed cases suggest a threshold value of about $r_0 = 10$ μm as in *TC80*, rather than 4.5 to 7.5 μm, as used in GCM. It also corroborates the results obtained by *Boers et al.* [1998] from the analysis of winter and summer stratocumulus clouds during SOCEX. *Boers et al.* [1998] estimate the auto-conversion threshold at 12–13 μm in mean droplet effective radius. The value considered here is MVDR at cloud top, which is slightly smaller than the effective radius at cloud top.

[41] *Gerber* [1996] proposed a substantially larger value for the critical radius, namely 16 μm in effective radius. The discrepancy in fact reflects a basic divergence in the definition of the critical radius. Here it represents the largest size droplets must reach in regions void a drizzle, which is before collection is active, for this process to be initiated. In *Gerber* [1996] it is derived from samples collected in regions where the collection process is already acting ($q_r > 0.01$ g m^{-3}) and it is biased by the few resulting big droplets.

[42] The onset of precipitation is dependent upon the formation of a few big droplets in the cloud layer. It might thus be expected that the maximum value of r_{95}, which characterizes the biggest droplets in the spectrum, should be a better predictor of drizzle formation than the maximum MVDR value. Figure 2 contradicts this assessment demonstrating that r_{vmax} is better suited for the diagnostic of the onset of precipitation. This result is crucial for the parameterization of precipitation formation in GCM. In fact, very little is known about the broadening of the droplet spectra, especially toward the large droplet sizes, and there is presently no parameterization available for the diagnostic of r_{95}, or any other characteristics of the large radius tail of

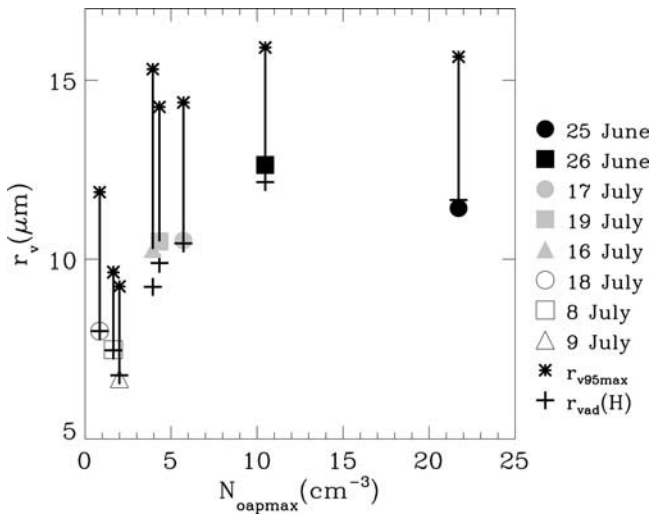

Figure 2. Maximum drizzle concentration for the eight ACE-2 cases versus maximum droplet sizes: r_{vmax} (symbols as indicated in the legend), r_{95max} (star), and $r_{vad}(H)$ (plus sign).

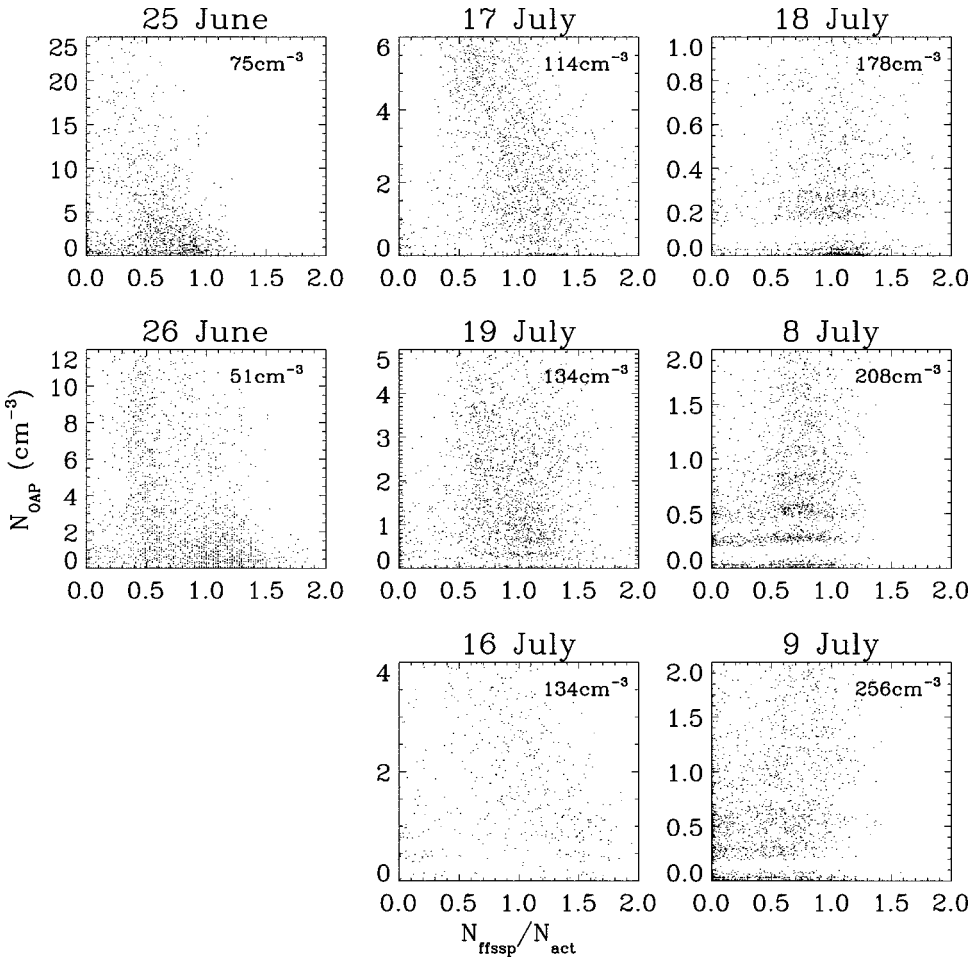

Figure 3. Scatterplot of 1 Hz samples of drizzle concentration versus droplet concentration normalized by N_{act}.

the droplet spectra. In contrast, the maximum MVDR value (at cloud top) can be calculated with the adiabatic model as a function of H and N, and Figure 2 demonstrates that such an adiabatic predictions $r_{vad}(H)$ closely agrees with the measured maximum value r_{vmax}.

[43] The examination of Figure 2 raises an important question: N_{OAPmax} is obviously larger in pristine than in polluted clouds. Does that mean that the precipitation process is more efficient? The question could be addressed by considering both the number concentration of drizzle and its size distribution, as for the characterization of cloud droplets. An alternative approach is to consider how drizzle affects the droplet distributions by collection, as suggested in Section 1. In Figure 3 N_{OAP} values are plotted for each 1 Hz sample versus the CDNC value in that sample, normalized by the CDNC value characteristic N_{act}. For the two pristine cases, the largest N_{OAP} values are observed in samples with low values of N/N_{act}, down to 0.2. This feature suggests that droplet collection by drizzle particles is active in these two pristine cloud layers. However, in the three most polluted cases, with much lower N_{OAP} values, the N_{OAP} peak values are observed in samples with N/N_{act} close to 1. This feature suggests that the particles observed with the 0AP-200X are in fact big droplets formed in active cloud cores, which are not efficient at depleting the smaller numerous cloud droplets. The three partially polluted cases exhibit intermediate features.

5.2. Bulk Parameterization of the Precipitation Process

[44] When observed with the fine resolution of airborne measurements, with ground or airborne millimetric radars [*Vali et al.*, 1998], or simulated with a CRM, a stratocumulus layer shows a large variety of microphysical structures: quasi-adiabatic cloud cores with narrow droplet spectra, very localized and short-lived regions of transition from droplets to drizzle drops, and isolated areas of precipitation, also called virga, extending from the top to below cloud base. The lifetime of such structures is of the order of a few tens of minutes. It can thus be anticipated that a GCM, with a spatial resolution of the order of 100 km and a time resolution longer than 20 min, is not capable of simulating explicitly the sequence of these microphysical stages. An interesting issue then is to examine if, at the large scale, the cloud layer reaches a nearly steady state, with a characteristic time of evolution of the order of the GCM time step. The analysis is a priori restricted to the cloudy part of the sampled area, the cloud fraction being considered as an issue to address separately.

[45] The examination of Table 1 reveals that the cloud fraction F_c varies from 50% (9 July) to 88% (17 July).

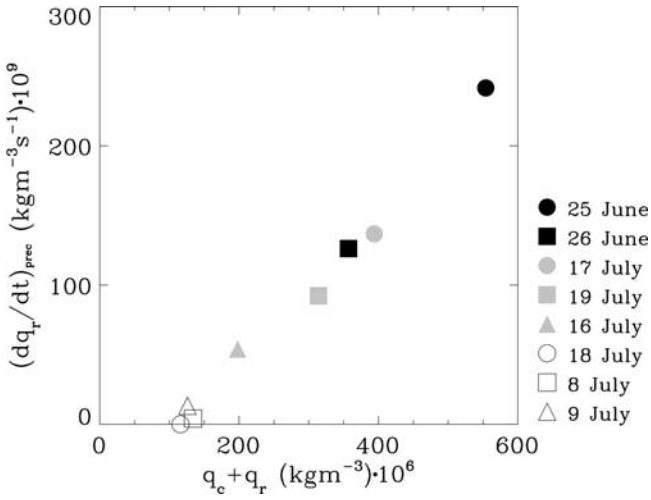

Figure 4. Drizzle reduction rate by precipitation versus total LWC.

Drizzle is detected in a smaller fraction of the sampled area, with a ratio F_r/F_c that varies from negligible values in the polluted cases, up to 0.47 on 17 July. Figure 4 shows the drizzle reduction rate by precipitation $(dq_r/dt)_{prec}$ (section 4.4) plotted versus the total (droplets and drizzle drops) water content, $q_c + q_r$. In nonprecipitating clouds, namely the three polluted cases, the total LWC is reduced to q_c, and it shows values between 60% (18 July) and 70% (8 July) of the predicted mean adiabatic LWC, $\overline{q_{ad}}$. Indeed the mean adiabatic droplet LWC prediction is based, according to equation (3), on the geometrical thickness H that corresponds to the deepest cells observed in the layer (section 4.1). This result thus suggests that the variability of the cloud thickness and the diluting effect of mixing result statistically in mean LWC values of about 60 to 70% of an adiabatic prediction based on the thickness of the deepest cells. In precipitating clouds the total water content increases with the precipitation flux, up to values almost two times higher than the adiabatic prediction. This feature reflects the fact that drizzle water is accumulated in the cloud layer until its precipitation flux compensates the conversion of cloud to rainwater. It is interesting though to notice that the 26 June case, despite its lower thickness value (202 m), accumulates almost the same amount of total LWC (0.357 g m^{-3}) as the 17 July, with 272 m and 0.394 g m^{-3}, for H and total LWC, respectively.

[46] If the cloud layer reaches a nearly steady state, the drizzle reduction rate $(dq_r/dt)_{prec}$ shall be equal to the drizzle production rate, $(dq_r/dt)_{aut} + (dq_r/dt)_{acc}$. This later quantity is estimated using the measured N_{act}, q_c and q_r values with three parameterizations, from *TC80*, as reported in equations (5) and (7), and from *KK00*, using either the same equations as *TC80*, but different values of the auto-conversion and accretion coefficients as indicated in section 3.2, or their ''best fits'' reported in equations (6) and (8) for accretion and auto-conversion, respectively. The values calculated for the eight ACE-2 cases are reported in Table 1, with the labels *TC*, *KK1*, and *KK2*, respectively. The measured drizzle LWC reduction rate by precipitation $(dq_r/dt)_{prec}$ is compared to these three parameterization diagnostics in Figure 5. The agreement is remarkable, especially for the *KK1* parameterization. The LWC values of Table 1 are cloud system mean values that are lower than the local peak values, especially for drizzle water content that is detectable over less than half of the cloud fraction (F_r/F_c). The concordance between the in situ measured reduction rate and the calculated production rate is therefore surprising, when considering the nonlinearity of the microphysical processes and the fact that the parameterizations were tuned against explicit microphysics calculations that are valid for local values. In fact q_c is sufficiently uniform within the cloud fraction, for $(dq_r/dt)_{aut}$ and $(dq_r/dt)_{acc}$ to behave like quasi-linear functions of q_r. This peculiarity could justify the use of CRM parameterizations in GCM, at least in stratocumulus clouds where the spatial variability of the cloud LWC is less pronounced than in deep cumulus clouds.

[47] Table 1 also shows that the contribution of auto-conversion in precipitating cloud systems (intermediate and pristine cases) is more than one order of magnitude smaller than the contribution of accretion. This feature emphasizes the difference between the onset of precipitation and its production. In CRM the onset of precipitation is parameterized with the auto-conversion process, while the production of precipitation results mainly from accretion. In large-scale models the onset of precipitation can be accounted for by comparing the critical radius value to a diagnostic of maximum MVDR based on H and N, as a surrogate for auto-conversion. However, the data set analyzed here suggests that the production of precipitation shall be accounted for by a large-scale parameterization of collection, thus implying that climate models ''tuning'' should be performed on accretion parameterization rather than auto-conversion. There is however a significant difference between the two CRM schemes since auto-conversion only involves q_c, while accretion involves both q_c and q_r. Does that mean that the extrapolation of the CRM schemes to GCM requires a diagnostic of the drizzle water content?

5.3. Grid Scale Diagnostic of the Precipitation Rate

[48] In Table 1 it is apparent that the precipitation flux R is the lowest in the polluted cases and that it increases as

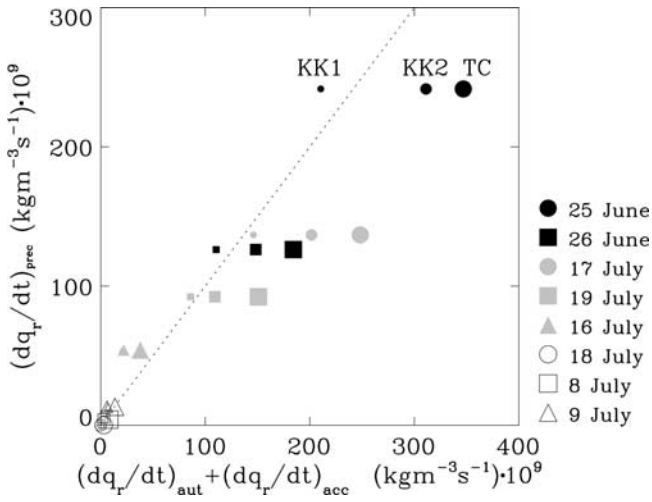

Figure 5. Drizzle reduction rate by precipitation versus total drizzle production rate (auto-conversion and accretion) as derived from CRM parameterizations (see section 5.2) initialized with the measured cloud and drizzle LWC.

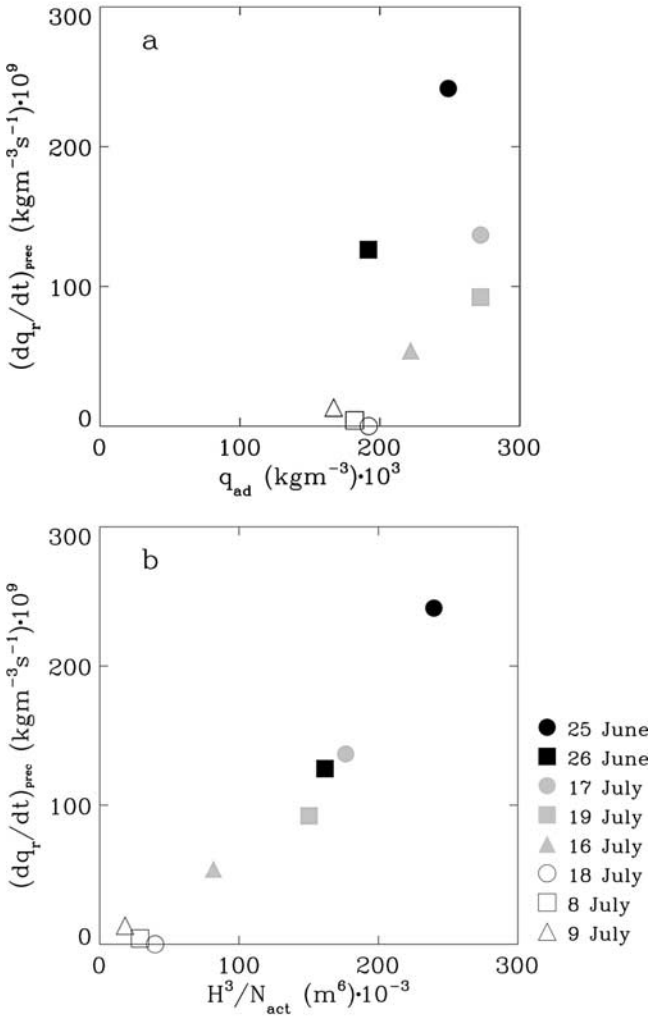

Figure 6. Drizzle reduction rate by precipitation versus adiabatic prediction of (a) mean adiabatic LWC versus (b) H^3/N_{act}.

CDNC decreases, up to a value of 0.0633 g m^{-2} s^{-1}, which is ~5.5 mm per day. It is also interesting to note that the 26 June case, though it exhibits the lowest N_{act} value and the biggest droplet sizes, does not correspond to the largest precipitation flux. This feature illustrates the differences between two important parameterization concepts. On the one hand, the onset of precipitation, depends upon the ability of the cloud to produce big droplets acting as precipitation embryos. On the other hand, the precipitation flux depends mainly, once precipitation started, upon the available LWC that is upon cloud depth. The size of the biggest droplets is proportional to $(H/N)^{1/3}$, hence the 26 June case, with H/N = 202/51 ~ 4, shows bigger droplets (r_{vmax} = 12.6 μm), than the 25 June case, with H/N = 262/75 ~ 3.5, (r_{vmax} = 11.4 μm). However, the mean LWC is proportional to H. Therefore the 25 June case, with H = 262 m, exhibits a larger precipitation flux (R = 0.0633 g m^{-2} s^{-1}), than the 26 June case, with a lower cloud depth, H = 202 m (R = 0.0255 g m^{-2} s^{-1}). In the series of intermediate cases, 17 July shows the greatest precipitation flux because of its large cloud thickness. 19 July shows about the same precipitation flux as 26 June, though its N_{act} value is substantially larger. This is due to its greater cloud depth, 272 m compared to 202 m in the 26 June case. 16 July, with a low cloud depth and a high N_{act} value shows the lowest precipitation flux. For the three polluted cases, the cloud depth is lower and the N_{act} value is higher than for the pristine and intermediate cases. Therefore the maximum MVDR values do not exceed the auto-conversion threshold and these three cases exhibit negligible precipitation fluxes.

[49] The final step thus consists in the examination of how the measured drizzle reduction rate $(dq_r/dt)_{prec}$ scales with H and N only. Figure 6a shows drizzle reduction rate $(dq_r/dt)_{prec}$ versus the predicted adiabatic mean LWC ($\propto H$). A broad scatter is observed, with the pristine cases showing higher $(dq_r/dt)_{prec}$ to $\overline{q_{ad}}$ ratios than the intermediate cases. However, a linear relationship is obtained in Figure 6b, where $(dq_r/dt)_{prec}$ is plotted versus H^3/N_{act}. It can be expressed as

$$(dq_r/dt)_{prec} = C_R\left[H^3/N_{act} - \left(H^3/N_{act}\right)0\right],$$

$$\text{with } C_R = 10^{-6} \text{ and} \left(H^3/N_{act}\right)_0 = 0.043. \qquad (12)$$

This result is particularly interesting for the 26 June against 19 July cases, that show very different H/N values (202/51 for 26 June, 272/134 for 19 July), but comparable precipitation fluxes.

6. Conclusion

[50] The ACE-2 CLOUDYCOLUMN data set has been analyzed with emphasis on the formation of precipitation. The main difference between the present study and the previous ones is in the characterization of the cloud layer as a whole. In previous studies [*Martin et al.*, 1994; *Gerber*, 1996; *Boers et al.*, 1998] attention was focused on local correlations between physical parameters. Further, the observed properties were merged to form an ensemble view of the cloud systems, each being represented by a subpopulation of data points. The approach developed here is different in the sense that each case is first examined and processed to retrieve properties that are representative of the cloud system at the scale of a GCM grid. Parameters representative of the aerosol activation process, such as the droplet concentration in regions unaffected by mixing or drizzle scavenging, and of the cloud layer morphology, such as the cloud system geometrical thickness, are derived with robust statistical procedures applied to the numerous ascents and descents flown through the cloud layer. Mean values over the cloud fraction of the sampled area are also derived for parameters used in bulk parameterizations, such as droplet and drop water contents, and mean precipitation flux. The analysis then focuses on differences between these cloud system values for the eight ACE-2 cases.

[51] The main obstacle in the characterization of a cloud layer is the high spatial variability of the microphysics and its stratification along the vertical. Because cloud base and top are also varying spatially, horizontal legs at constant altitude are difficult to interpret statistically. They generally introduce a bias toward values specific of that altitude. In contrast the global approach developed here is based on a large number of cloud profiles, either ascents or descents,

flown on each case, with at least 15, and up to 35 profiles. Another unique feature of the data set is that the eight cases reflect a large range of aerosol properties, with pristine aerosol (2 cases), intermediate (3 cases) and polluted aerosol (3 cases). The CDNC value representative of the aerosol activation process (N_{act}) ranges from 50 to 250 cm^{-3}, hence providing a reference data set for the study of both the first and second aerosol indirect effects. Last the instrumented aircraft flew a 60 km square pattern, a dimension that is well suited for comparison with GCM grids. The main results are summarized here:

[52] 1. Current estimations of the critical radius for auto-conversion in GCM are based on the grid mean LWC, and a smaller value of the critical radius is used, as in *Boucher and Lohmann* [1995], *Rasch and Kristjansson* [1998], or *Rotstayn* [1999], to compensate for the coarse spatial resolution. The ratio of the grid mean LWC to its peak value at the top of adiabatic cores however is not a universal constant. It rather depends on the cloud dynamics and the microphysics spatial heterogeneities. The rationale for using grid mean values of LWC, hence of MVDR, is not supported by CRM simulations with explicit microphysics, which rather suggest that the onset of precipitation depends on local MVDR peak values, which are produced close to cloud top. The experimental analysis of the drizzle maximum number concentration versus MVDR reveals that the onset of precipitation is dependent upon the maximum MVDR value in the cloud system, and that a threshold value of 10 μm, as previously used in CRM [*TC80*], is appropriate. An important point to notice is that MVDR is derived from statistics based on samples void of drizzle drops. Otherwise the critical radius estimation is biased by the presence of a few big droplets that are produced by collection of the droplets and drops. The value proposed here shall thus be interpreted as the maximum size droplets must reach in a cloud for the precipitation process to be activated. The analysis also demonstrates that the observed maximum MVDR is well predicted with the adiabatic model, using the cloud system characteristic values H and N_{act}.

[53] 2. A clear identification is made of cloud systems where droplet collection is efficient by examination of the correlation between drizzle number concentration and the ratio of CDNC to N_{act}, in 90 m long samples. The two pristine cases, and partly the intermediate cases, exhibit substantial CDNC reduction by droplet collection, while the three polluted cases exhibit smaller drizzle concentrations and predominantly in association with comparable or larger CDNC values than N_{act}.

[54] 3. The drizzle reduction rate by precipitation was derived from 90 m samples by integration over the drizzle spectrum, and then averaged over the sampled area. In order to evaluate if the stratocumulus reaches a nearly steady state, this rate is compared to the drizzle production rate by auto-conversion and accretion, as derived from parameterizations initialized with the measured cloud and drizzle water contents. Three parameterizations are tested, one from *TC80* and two from *KK00*. The agreement between the measured reduction rate by precipitation and the parameterized production rate is remarkable for the first *KK00* parameterization. This result suggests that nonlinearity of the processes does not prevent estimation of the precipitation rate at the large scale. Indeed the cloud LWC is sufficiently uniform within the cloud layer for both the auto-conversion and the accretion parameterizations to behave like quasi-linear functions of drizzle LWC.

[55] 4. At the cloud system scale and only if the auto-conversion critical radius is reached (the intermediate and pristine cases in Table 1), the contribution of auto-conversion to the drizzle production is less than one order of magnitude smaller than the contribution of accretion. This suggests that GCM models should be tuned via the accretion parameterization rather than focusing on the auto-conversion scheme.

[56] The ultimate objective is to evaluate if a large-scale parameterization of the precipitation process in boundary layer clouds is feasible, using only two large-scale parameters, namely H and N_{act}. It appears that the drizzle reduction rate by precipitation for the eight analyzed cases is accurately represented by a H^3/N_{act} power law, as reported in equation (12). It would be interesting now to challenge such a simplification against other data sets and large eddy simulations of boundary layer clouds with explicit microphysics. These results are only valid for the cloudy part of the sampled area; the determination of the cloud fraction is also a crucial issue that needs to be addressed separately.

[57] The ACE-2 analysis suggests that the precipitation process in extended boundary layer clouds could be treated in GCM with a diagnostic scheme based on only H and N_{act}, for deriving the maximum MVDR to compare to the critical radius for the onset of precipitation, and for calculating the precipitation rate in the layer. N_{act} can be predicted in GCM, based on parameterizations of the aerosol activation process, such as discussed by *Zhang et al.* [2002]. H in contrast is poorly diagnosed because of the coarse vertical resolution of GCM in the boundary layer. However, the result presented here emphasizes the crucial importance of the cloud geometrical thickness for the formation of precipitation ($\propto H^3$). Similarly, *Brenguier et al.* [2000a] showed that cloud optical thickness is proportional to $H^{5/3}$. A very significant step would thus be to improve the prediction of cloud geometrical thickness in GCM. An approach based on vertical subgrid diagnostic of cloud geometrical thickness [*Lock et al.*, 2000] is an interesting complement to the refinement of the vertical resolution.

[58] **Acknowledgments.** The authors acknowledge the help of the members of the PACE group. Their contributions to the data analysis and interpretation and to the editorial work are most appreciated. This work is supported by the European Union under grant EVK2-CT-1999-00054, by the Polish State Committee for Scientific Research (KBN) under grant SPUB-M, by Météo-France and CNRS.

References

Albrecht, B. A., Aerosols, cloud microphysics, and fractional cloudiness, *Science*, *245*, 1227–1230, 1989.

Bartlett, J. T., The effect of revised collision efficiencies on the growth of cloud droplets by coalescence, *Q. J. R. Meteorol. Soc.*, *96*, 730–738, 1970.

Beheng, K. D., A parameterization of warm cloud microphysical conversion process, *Atmos. Res.*, *33*, 193–206, 1994.

Berry, E. X., Cloud droplet growth by collection, *J. Atmos. Sci.*, *24*, 688–701, 1967.

Boers, R., J. B. Jensen, and P. B. Krummel, Microphysical and short-wave radiative structure of stratocumulus clouds over the Southern Ocean: Summer results and seasonal differences, *Q. J. R. Meteorol. Soc.*, *124*, 151–168, 1998.

Boucher, O., and U. Lohmann, The sulphate-CCN-Cloud albedo effect: A sensitivity study using two General Circulation Models, *Tellus, Ser. B*, *47*, 281–300, 1995.

Brenguier, J. L., Parameterization of the condensation process: A theoretical approach, *J. Atmos. Sci.*, *48*, 264–282, 1991.

Brenguier, J. L., and L. Chaumat, Droplet spectra broadening in cumulus clouds. Part I: Broadening in adiabatic cores, *J. Atmos. Sci.*, *58*, 628–641, 2000.

Brenguier, J. L., T. Bourrianne, A. Coelho, J. Isbert, R. Peytavi, D. Trevarin, and P. Wechsler, Improvements of droplet size distribution measurements with the Fast-FSSP, *J. Atmos. Oceanic. Technol.*, *15*, 1077–1090, 1998.

Brenguier, J. L., H. Pawlowska, L. Schüller, R. Preusker, J. Fischer, and Y. Fouquart, Radiative properties of boundary layer clouds: Droplet effective radius versus number concentration, *J. Atmos. Sci.*, *57*, 803–821, 2000a.

Brenguier, J. L., P. Y. Chuang, Y. Fouquart, D. W. Johnson, F. Parol, H. Pawlowska, J. Pelon, L. Schüller, F. Schröder, and J. R. Snider, An overview of the ACE-2 CLOUDYCOLUMN Closure Experiment, *Tellus, Ser. B*, *52*, 814–826, 2000b.

Brenguier, J.-L., H. Pawlowska, and L. Schuller, Cloud microphysical and radiative properties for parameterization and satellite monitoring of the indirect effect of aerosol on climate, *J. Geophys. Res.*, *108*(D15), 8632, doi:10.1029/2002JD002682, in press, 2003.

Feingold, G., B. Stevens, W. R. Cotton, and R. L. Walko, An explicit cloud microphysical/LES model designed to simulate the Twomey effect, *Atmos. Res.*, *33*, 207–233, 1994.

Feingold, G., W. R. Cotton, S. M. Kreidenweis, and J. T. Davis, The impact of giant cloud condensation nuclei on drizzle formation in stratocumulus: Implications for cloud radiative properties, *J. Atmos. Sci.*, *56*, 4100–4117, 1999a.

Feingold, G., A. S. Frisch, B. Stevens, and W. R. Cotton, On the relationship among cloud turbulence, droplet formation and drizzle as viewed by Doppler radar, microwave radiometer and lidar, *J. Geophys. Res.*, *104*, 22,195–22,203, 1999b.

Fowler, L. D., D. A. Randall, and S. A. Rutledge, Liquid and ice cloud microphysics in the CSU general circulation model. Part I: Model description and simulated microphysical processes, *J. Clim.*, *9*, 489–529, 1996.

Gerber, H., Microphysics of marine stratocumulus clouds with two drizzle modes, *J. Atmos. Sci.*, *53*, 1649–1662, 1996.

Ghan, S. J., L. R. Leung, and Q. Hu, Application of cloud microphysics to NCAR community climate model, *J. Geophys. Res.*, *102*, 16,507–16,527, 1997.

Guibert, S., J. J. Snider, and J.-L. Brenguier, Aerosol activation in marine stratocumulus clouds: 1. Measurement validation for a closure study, *J. Geophys. Res.*, *108*(D15), 8628, doi:10.1029/2002JD002678, in press, 2003.

Harrington, J. Y., G. Feingold, and W. R. Cotton, Radiative impacts on the growth of a population of drops within simulated summertime Artic stratus, *J. Atmos. Sci.*, *57*, 766–785, 2000.

Kessler, E., On the distribution and continuity of water substance in atmospheric circulations, *Meteorol. Monogr.*, *10*, 84 pp., 1969.

Khairoutdinov, M., and Y. Kogan, A new cloud physics parameterization in a large-eddy simulation model of marine stratocumulus, *Mon. Weather Rev.*, *128*, 229–243, 2000.

Kogan, Y. L., M. P. Khairoutdinov, D. K. Lilly, Z. N. Kogan, and Q. Liu, Modeling of stratocumulus cloud layers in a large eddy simulation model with explicit microphysics, *J. Atmos. Sci.*, *52*, 2923–2940, 1995.

Lock, A. P., A. R. Brown, M. R. Bush, A. L. M. Grant, G. M. Martin, and R. N. B. Smith, The impact of an improved representation of boundary layer mixing on the simulation of clouds in the Unified Model, paper presented at the World Climate Research Program (WCRP) Global Energy and Water Cycle Experiment (GEWEX) Workshop on Cloud Processes and Cloud Feedbacks in Large-Scale Models, 9–13 November 1999, WCRP-110; WMO/TD-NO. 993, pp. 42–51, World Meteorol. Org., Eur. Cent. for Medium-Range Weather Forecasts, Reading, U.K., 2000.

Lohmann, U., and E. Roeckner, Design and performance of a new cloud microphysics scheme developed for the ECHAM general circulation model, *Clim. Dyn.*, *12*, 557–572, 1996.

Martin, G. M., D. W. Johnson, and A. Spice, The measurement and parameterization of effective radius of droplets in warm stratocumulus clouds, *J. Atmos. Sci.*, *51*, 1823–1842, 1994.

Menon, S., A. D. DelGenio, D. Koch, and G. Tselioudis, GCM simulations of the aerosol indirect effect: Sensitivity to cloud parameterization and aerosol burden, *J. Atmos. Sci*, *59*, 692–713, 2002.

Pawlowska, H., and J. L. Brenguier, Microphysical properties of stratocumulus clouds during ACE-2, *Tellus, Ser. B*, *52*, 867–886, 2000.

Pruppacher, H. R., and J. D. Klett, *Microphysics of Clouds and Precipitation*, Kluwer Acad., Norwell, Mass., 1997.

Rasch, P. J., and J. E. Kristjánsson, A comparison of the CCM3 model climate using diagnosed and predicted condensate parameterisations, *J. Clim.*, *11*, 1587–1614, 1998.

Rotstayn, L. D., A physically based scheme for the treatment of stratiform clouds and precipitation in large-scale models. I: Description and evaluation of the microphysical processes, *Q. J. R. Meteorol. Soc.*, *123*, 1227–1282, 1997.

Rotstayn, L. D., Indirect forcing by anthropogenic aerosols: A global climate model calculation of the effective-radius and cloud-lifetime effects, *J. Geophys. Res.*, *104*, 9369–9380, 1999.

Rotstayn, L. D., On the "tuning" of auto-conversion parameterizations in climate models, *J. Geophys. Res.*, *105*, 15,495–15,507, 2000.

Schüller, L., J.-L. Brenguier, and H. Pawlowska, Retrieval of microphysical, geometrical and radiative properties of marine stratocumulus from remote sensing, *J. Geophys. Res.*, *108*(D15), 8631, doi:10.1029/2002JD002680, in press, 2003.

Snider, J. R., and J. L. Brenguier, A comparison of cloud condensation nuclei and cloud droplet measurements obtained during ACE-2, *Tellus, Ser. B*, *52*, 827–841, 2000.

Snider, J., S. Guibert, J.-L. Brenguier, and J.-P. Putaud, Aerosol activation in marine stratocumulus clouds: 2. Köhler and parcel theory closure studies, *J. Geophys. Res.*, *108*(D15), 8629, doi:10.1029/2002JD002692, in press, 2003.

Sundqvist, H., A parameterization scheme for the non-convective parameterization including prediction of cloud water content, *Q. J. R. Meteorol. Soc.*, *104*, 677–690, 1978.

Tiedtke, M., Representation of clouds in large-scale models, *Mon. Weather Rev.*, *121*, 3040–3061, 1993.

Tripoli, G. J., and W. R. Cotton, A numerical investigation of several factors contributing to the observed variable intensity of deep convection over south Florida, *J. Appl. Meteorol.*, *19*, 1037–1063, 1980.

Twomey, S., The influence of pollution on the shortwave albedo of clouds, *J. Atmos. Sci.*, *34*, 1149–1152, 1977.

Vali, G., R. D. Kelly, J. French, S. Haimov, and D. Leon, Fine scale structure and microphysics of coastal stratus, *J. Atmos. Sci.*, *55*, 3540–3564, 1998.

Wilson, D. R., and S. P. Ballard, A microphysically based precipitation scheme for the UK Meteorological Office Unified Model, *Q. J. R. Meteorol. Soc.*, *125*, 1607–1636, 1999.

Zhang, Y., R. C. Easter, S. J. Ghan, and H. Abdul-Razzak, Impact of aerosol size representation on modeling aerosol-cloud interactions, *J. Geophys. Res.*, *107*(D21), 4558, doi:10. 1029/2001JD001549, 2002.

J.-L. Brenguier, Centre National de Recherche Météorologique (CNRM), GMEI/D, Météo-France, F-31057 Toulouse Cedex 01, France. (jlb@meteo.fr)

H. Pawlowska, Institute of Geophysics, Warsaw University, ul. Pasteura 7, 02-093 Warsaw, Poland. (hanna.pawlowska@igf.fuw.edu.pl)